Journal of Molecular Catalysis A: Chemical 326 (2010) 82–87

Contents lists available at ScienceDirect

Journal of Molecular Catalysis A: Chemical

journal homepage: www.elsevier.com/locate/molcata

# Hydrodealkylation of 1,2,4-trimethylbenzene over reduced Ni–Al mixed oxide catalysts prepared by co-precipitation method

Zongwen Guo[a,b], Weitao Huo[a], Mingjun Jia[a], Kaige Li[a], Zhenlu Wang[a,*], Wenxiang Zhang[a,*]

[a] Key Laboratory of Surface and Interface Chemistry of Jilin Province, College of Chemistry, Jilin University, Qianjin Road 2699, Changchun, Jilin 130012, China
[b] College of Chemistry and Environment Engineering, Harbin University of Science and Technology, Xuefu Road 52, Harbin 150010, China

ARTICLE INFO

*Article history:*
Received 22 December 2009
Received in revised form 20 April 2010
Accepted 22 April 2010
Available online 18 May 2010

*Keywords:*
Hydrodealkylation
1,2,4-Trimethylbenzene
Nickel aluminate
Pseudo-spinel

ABSTRACT

The hydrodealkylation of 1,2,4-trimethylbenzene (1,2,4-TMB) was investigated on partially reduced Ni–Al mixed oxide catalysts prepared by the co-precipitation method. The catalytic performances of these Ni–Al mixed oxides were considerably influenced by different factors, such as the molar ratio of Ni/Al, calcination temperature of the catalysts, etc. The sample with a Ni/Al molar ratio of 1:8 calcined at 500 °C (denoted as $NiAl_8$-500) showed the highest activity and total selectivity to lighter aromatics with a 62.3% conversion and a 60.2% selectivity to xylene. Characterization results showed that the unreduced $NiAl_8$-500 catalyst mainly consisted of pseudo-spinel like solid solution ($NiAl_2O_4$), and could produce monodispersed nickel atoms (Ni(0)), which are closely associated with alumina sites (Lewis acid) upon reduction. We propose that the relatively high hydrodealkylation activity of the $NiAl_8$-500 catalyst could be mainly assigned to the presence of a number of neighboring metallic Ni(0) atoms and Lewis acidic sites.

© 2010 Elsevier B.V. All rights reserved.

## 1. Introduction

Catalytic transformation of $C_9^+$ heavy aromatics to lighter aromatics of benzene, toluene and xylene (BTX) has been an interesting research subject for a long time because of the important application of BTX in chemical industry [1]. Hydrodealkylation is a major method for the utilization of heavy aromatics. A variety of catalysts, including supported transitional metal oxides and zeolite catalysts, have been widely investigated for the hydrodealkylation of $C_9^+$ heavy aromatics [2–7]. Among them, supported $Cr_2O_3/Al_2O_3$ is one of the most efficient catalyst systems, and several commercial processes based on this catalyst have been developed successfully. Recently, with the increase in concern over environmental protection, more attention was focused on developing novel and environmental benign catalysts with higher activity and selectivity to xylene (one of the most valuable product in lighter aromatics) for the hydrodealkylation of $C_9^+$ heavy aromatics.

Supported Ni based catalysts have been extensively used in industry due to their relatively high activity in catalytic hydrogenation reactions [8–11]. It was reported that the catalytic property of the supported Ni catalysts depends on various parameters, such as the nature of the support and the dispersion state of the active phase, as well as the interaction between Ni species and the support [12–15]. For a given support, i.e., alumina, it was known that Ni species could disperse on the surface of alumina, or diffuse into the bulk structure of $Al_2O_3$ to different extents, depending on the intrinsic properties of the support, Ni loading, and preparation parameters (methods, calcination temperatures, reduction conditions, etc.). A few recent works suggested that a kind of surface nickel spinel phase or pseudo-spinel phase ($NiAl_2O_4$) may be formed in the alumina-supported Ni catalysts by controlling the preparation factors [16–19]. This phase is between bulk nickel aluminate and nickel oxide in terms of interaction with the support, and may be a suitable compromise with respect to reducibility and stability for a given catalytic reaction. For instance, Sueiras and co-workers reported that high surface area $NiAl_2O_4$ spinels could be prepared by the co-precipitation method, and the reducibility of the spinels could be varied by changing the precipitation conditions and calcination temperatures of nickel aluminum hydroxide precursors of the spinels [20]. They believed that the spinels, which can be surface reduced, may be used in systems of catalytic interest in hydrogenation reactions and in the preparation of more resistant reduced catalysts. Kordulis and co-workers [21] found that highly active $Ni/Al_2O_3$ catalysts for the hydrogenation of benzene could be obtained by using sol–gel technique and co-precipitation method, and proposed that the suitable preparation methodology could ensure the best compromise between dispersion of the nickel phase and its interaction with the support surface to form active surface nickel spinel phase.

In the present work, we prepared a series of Ni–Al mixed oxides with spinel phase characteristics by means of co-precipitation, and investigated the influence of various preparation parameters (i.e.,

* Corresponding authors. Tel.: +86 431 85155390; fax: +86 431 88499140.
*E-mail addresses:* wzl@jlu.edu.cn (Z. Wang), zhwenx@jlu.edu.cn (W. Zhang).

1381-1169/$ – see front matter © 2010 Elsevier B.V. All rights reserved.
doi:10.1016/j.molcata.2010.04.011

Ni/Al ratio, calcination temperature) on their catalytic properties in the hydrodealkylation of 1,2,4-trimethylbenzene (1,2,4-TMB). It was well known that 1,2,4-TMB is the major component in $C_9^+$ heavy aromatics originating from the catalytic reforming process. As far as we know, most recent work was mainly drawn on the study of various catalytic transformation processes of 1,2,4-TMB, including isomerization, disproportionation and dealkylation over different solid acid catalyst systems (e.g., zeolites). However, few papers in open literature were reported concerning the hydrodealkylation of 1,2,4-TMB. Here, 1,2,4-TMB was chosen as a model compound for studying the hydrodealkylation $C_9^+$ heavy aromatics, and a variety of characterization means, including XRD, TPR, FTIR, UV-DRS and $NH_3$-TPD, were also employed in order to correlate their catalytic performance with the physicochemical properties of the Ni–Al mixed oxide catalysts.

## 2. Experimental

### 2.1. Catalysts preparation

The nickel aluminate precursors were prepared by co-precipitating a stoichiometric mixture of nickel nitrate and aluminum nitrate solutions according to a literature procedure [22]. The base (0.6 M aqueous $NH_3$) was added at 2 mL/min with constant stirring until the pH was varied from 4 to 8.5. After the precipitation, samples were aged for 24 h at room temperature. The precipitated materials were then filtered, washed with distilled water five times, and dried in an oven at 90 °C for 12 h. The crude products were calcined for 5 h at 500 °C, 700 °C or 900 °C, respectively. The resulting samples were designated as $NiAl_x$-$y$, where $x$ is the molar ratio of Ni/Al, and $y$ stands for the calcination temperature.

For comparison, a reference sample was prepared by supporting additional 1.0 wt% Ni on the sample of $NiAl_8$-700 via a wetness impregnation route. Typically, a weighted amount of the support was impregnated with nickel nitrate solution of a volume equal to its pore volume at room temperature. The impregnated solids were dried at 90 °C for 12 h, and then calcined at 500 °C for 5 h. The resulting samples were designated as $NiAl_8$-700IMP hereafter.

### 2.2. Characterization

X-ray diffraction (XRD) measurements of the samples were carried out on a Rigaka D max-2550 diffractometer using nickel-filtered Cu Kα radiation (λ = 1.54 Å). $N_2$ adsorption/desorption isotherms were measured at −196 °C, using a Micromeritics ASAP 2020M analyzer. Specific surface areas were calculated using the BET model. Pore size distributions were evaluated from desorption branches of nitrogen isotherms by using the BJH model. The FTIR spectra of the samples were recorded on an Avatar 370 infrared apparatus with KBr pellets in the range of 400–4000 $cm^{-1}$. Diffuse reflectance spectroscopy measurements were performed on a Rigaku UV-3100 spectra photometer in the range of 200–800 nm on a $BaSO_4$ plate. The TPR of the samples was performed in a flow system. 50 mg of the sample was treated in a flow of argon at 100 °C for 1 h. It was then heated to 900 °C under the $H_2$/Ar (5% $H_2$) atmosphere at a temperature ramping rate of 10 °C/min. Hydrogen consumption was measured with a TCD in a Shimadzu GC-8A chromatograph. The $NH_3$-TPD of the samples was carried out by a flow system. The catalyst (50 mg) was outgassed in argon flow, heated to 600 °C at rate of 10 °C/min, and kept at 600 °C for 1 h. The sample was cooled down to 50 °C and allowed to adsorb by ammonia. After purging the physically adsorbed ammonia, the system was heated to 600 °C under the argon flow. The amount of chemisorbed ammonia was detected with a TCD in a Shimadzu GC-8A gas chromatograph.

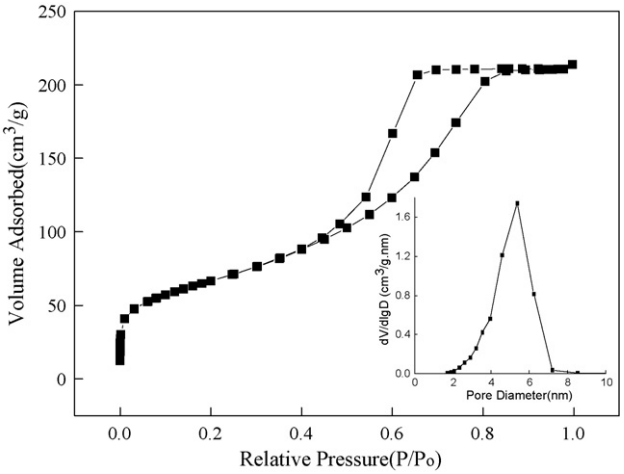


**Fig. 1.** $N_2$ adsorption–desorption isotherms and pore size distribution (inset) of $NiAl_8$-500.

### 2.3. Catalytic activity

Hydrodealkylation of 1,2,4-TMB was performed in a computer-controlled down-flow fixed-bed stainless steel tubular microreactor with an axial thermocouple and heated in a one-zone electrical furnace. The reactor was in sandwich charged with 0.7 g of catalysts diluted with carborundum (SiC/zeolite volume ratio = 1) and filled carborundum at the inlet and outlet, respectively. The catalyst was in situ reduced at 550 °C for 1 h, then cooled down to the corresponding reaction temperature (450 °C) in a flow of pure hydrogen (flow rate = 50 mL/min). The catalytic test was carried out under the condition of 3.0 MPa with $H_2$/1,2,4-TMB molar ratio of 1.9 (LHSV = 1.1 $h^{-1}$). The products and reactants were analyzed online by a Shimadzu GC-14B gas chromatograph equipped with an FID detector and DB-wax capillary column (60 m, 0.35 mm i.d., 0.5 μm). In all tests, mass and carbon balances were within 100 ± 5%.

## 3. Results and discussion

### 3.1. Catalyst characterization

Table 1 shows the preparation parameters and physical data of various Ni–Al mixed oxide catalysts. It can be seen that all the samples possess relatively high surface areas, except for the sample $NiAl_8$-900 calcined at high temperature. The $N_2$ adsorption–desorption isotherms and pore size distribution of a representative sample ($NiAl_8$-500) are given in Fig. 1. It shows a typical type IV isotherm (definition by IUPAC), which is a characteristic of mesoporous materials. Besides, this sample possesses well-developed framework porosity with narrow pore size distribution centered at 5.4 nm [23].

The XRD patterns of various Ni–Al mixed oxide catalysts with different Ni/Al molar ratios (calcined at 500 °C) are shown in Fig. 2A. All the samples exhibit similar diffraction lines at 2$\theta$ values of 37°, 45° and 65°, which could be assigned to a spinel or pseudo-spinel structure [24]. The black coloration of the two samples $NiAl_2$-500 and $NiAl_4$-500 implies that the co-existence of a certain amount of nickel oxides, although no diffraction peaks of crystalline NiO are found in their XRD patterns. The $NiAl_8$-500 sample shows a green coloration, which can be attributed to the formation of a jasper pseudo-spinel phase. With the further decrease in the Ni/Al ratio (i.e., 1/16), the coloration $NiAl_{16}$-500 turns blue, suggesting the phase change from pseudo-spinel to spinel. On the basis of related literatures, it can be concluded here that the Al-rich sample mainly consists of spinel-type γ-$Al_2O_3$ and $NiAl_2O_4$ phases.

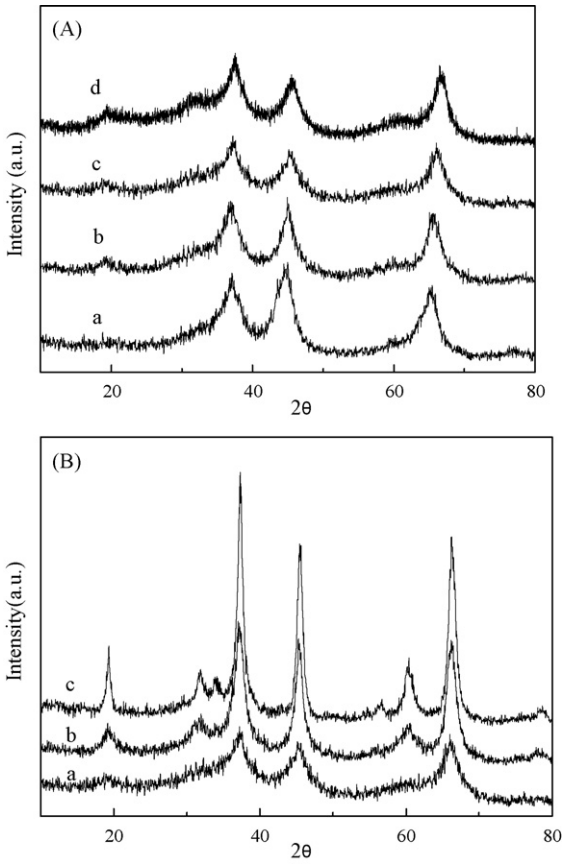


**Fig. 2.** XRD patterns of $NiAl_2$-500 (a), $NiAl_4$-500 (b), $NiAl_8$-500 (c) and $NiAl_{16}$-500 (d) (A). XRD patterns of $NiAl_8$-500 (a), $NiAl_8$-700 (b) and $NiAl_8$-900 (c) (B).

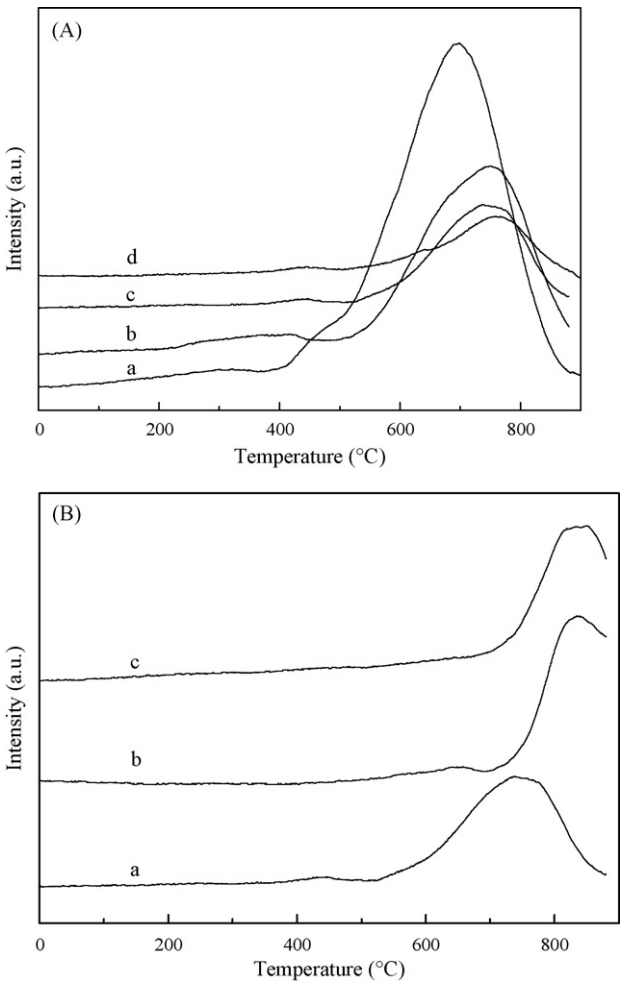


**Fig. 3.** TPR profiles of $NiAl_2$-500 (a), $NiAl_4$-500 (b), $NiAl_8$-500 (c) and $NiAl_{16}$-500 (d) (A). TPR profiles of $NiAl_8$-500 (a), $NiAl_8$-700 (b) and $NiAl_8$-900 (c) (B).

Fig. 2B shows the XRD patterns of the samples with Ni/Al = 1/8 calcined at different temperatures. For the samples $NiAl_8$-700 and $NiAl_8$-900, the diffraction peaks at 2$\theta$ values of 19°, 32°, 37°, 45°, 59° and 65° can be attributed to the spinel phase $NiAl_2O_4$ which were consistent with those of standards taken from JCPDS. Compared to the sample $NiAl_8$-500, a slight shift in the diffraction lines toward higher 2$\theta$ could be observed on the samples calcined at higher temperatures ($NiAl_8$-700 and $NiAl_8$-900), implying the phase transformation from pseudo-spinel to spinel occurs when the calcination temperatures increase [22,24]. This point can be further confirmed by the coloration change from green to blue with increasing calcination temperature. For the sample $NiAl_8$-900, two additional weak peaks at 34° and 56° might be associated with the formation of some kinds of crystal phase of $\gamma$-$Al_2O_3$.

The reducibility of various Ni–Al catalysts is investigated by $H_2$-TPR measurements. The samples with different Ni/Al molar ratios (calcined at 500 °C) show a weak peak around 400 °C, and a strong peak in a broad range of 500–900 °C (Fig. 3A). The low-temperature peak can be assigned to the reduction of a trace amount of NiO, which should be highly dispersed on the surface of the catalyst. The reduction temperature of such kinds of NiO species is slightly higher than that of crystallized NiO as reported in related literature [25], suggesting the presence of very weak interaction between NiO species and supports ($Al_2O_3$ or $NiAl_2O_4$). The strong peak at high temperature may correspond to the reduction of $Ni^{2+}$ present in different surroundings, i.e., surface pseudo-spinel and bulk spinel $NiAl_2O_4$. With the decrease in the Ni/Al ratio, this reduction peak shifts to higher temperatures slightly [26]. It should be mentioned here that the reduction of $NiAl_2O_4$ phase starts just at about 530 °C, which is much lower than the reduction temperature of the sample prepared by the conventional method [21]. For the samples with Ni/Al = 1/8 calcined at different temperatures, it can be seen that the high-temperature reduction peak shifts from 750 to 850 °C when the calcination temperature of the catalyst increases from 500 to

**Table 1**
The main characteristics results of the catalysts.

| Catalysts | Ni/Al (mol/mol) | Calcination temp. (°C) | Surface area ($m^2$/g)[a] | Average pore diameter (nm)[b] | Color |
|---|---|---|---|---|---|
| $NiAl_2$-500 | 1/2 | 500 | 240.9 | 5.50 | Black |
| $NiAl_4$-500 | 1/4 | 500 | 241.2 | 5.92 | Black |
| $NiAl_8$-500 | 1/8 | 500 | 253.1 | 5.54 | Green |
| $NiAl_{16}$-500 | 1/16 | 500 | 271.8 | 5.64 | Green |
| $NiAl_8$-700 | 1/8 | 700 | 164.2 | 10.4 | Blue |
| $NiAl_8$-900 | 1/8 | 900 | 65.8 | 17.0 | Light blue |

[a] BJH adsorption surface area.
[b] BJH adsorption average pore diameter.

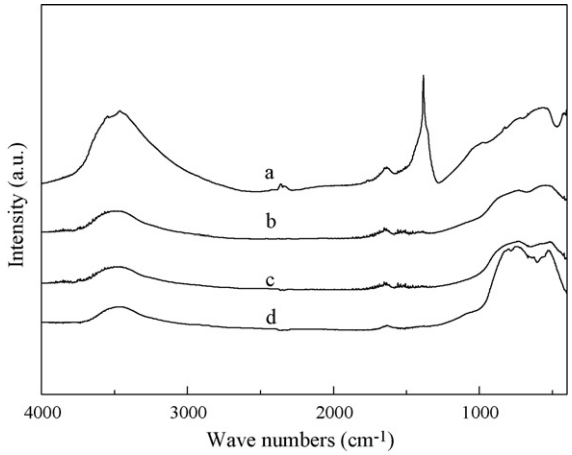


**Fig. 4.** FTIR spectrum of precursor (a), $NiAl_8$-500 (b), $NiAl_8$-700 (c) and $NiAl_8$-900 (d).

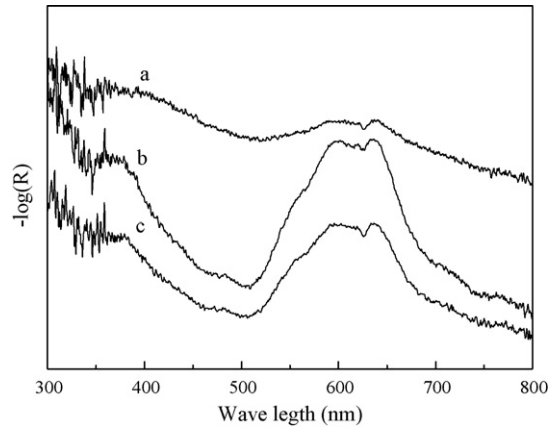


**Fig. 5.** UV-DRS profiles of $NiAl_8$-500 (a), $NiAl_8$-700 (b) and $NiAl_8$-900 (c).

700 °C (or 900 °C). Meanwhile, the low-temperature reduction peak turns weaker and weaker with the increase in calcination temperature, and nearly disappears when the sample is calcined at 900 °C (Fig. 3B). These results suggest that the reducibility of Ni–Al mixed oxides are varied with the change of Ni/Al ratios and the calcination temperatures. Samples calcined at lower temperatures (i.e., 500 °C), is easier to reduce compared to the samples calcined at higher temperatures.

The FTIR spectra of the precursor of the catalyst (without calcination) as well as the calcined samples of $NiAl_8$-500, $NiAl_8$-700 and $NiAl_8$-900 are shown in Fig. 4. The spectrum of the catalyst precursor shows typical characteristics of LDH (layered double hydroxides) [27]. The strong absorption band at ca.1390 $cm^{-1}$ is probably attributed to the mode of nitrate and carbonate anions. The band at about 1000 $cm^{-1}$ can be attributed to nitrate and/or to M-OH modes (M = Ni, Al). The band at 602 $cm^{-1}$ of the precursor is attributed to Al–O for octahedrally coordinated aluminate ions. For the calcined samples of $NiAl_8$-500, $NiAl_8$-700 and $NiAl_8$-900, two broaden absorption vibrations at 722 and 602 $cm^{-1}$ were observed. According to the related literature [27–29], the band at 722 $cm^{-1}$ could be mainly assigned to the bending vibration mode of tetrahedrally coordinated Al–O, and the band at 602 $cm^{-1}$ to the stretching vibration mode of Al–O for the octahedrally coordinated aluminum ions. The coordination environments of the nickel and aluminum species are also characterized by UV-DRS (Fig. 5). The UV-DRS profiles are quite similar for the three catalysts of $NiAl_8$-500, $NiAl_8$-700 and $NiAl_8$-900. The band in the range of 600–645 nm

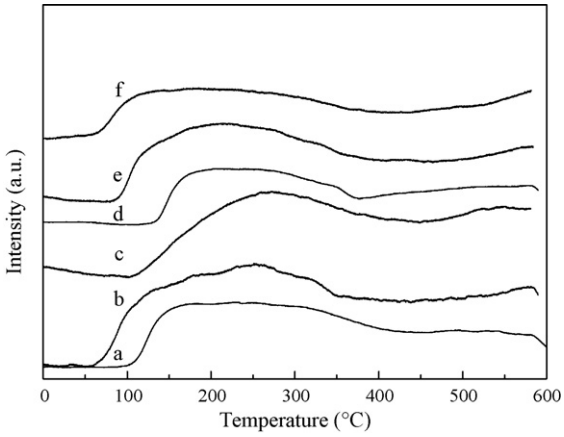


**Fig. 6.** NH3-TPD curve of $NiAl_2$-500 (a), $NiAl_4$-500 (b), $NiAl_8$-500 (c), $NiAl_{16}$-500 (d), $NiAl_8$-700 (e) and $NiAl_8$-900 (f).

could be attributed to the tetrahedral $Ni^{2+}$ species incorporated into the nickel aluminate lattice, and the two bands at 715 nm and 377 nm represent the presence of octahedrally coordinated $Ni^{2+}$ species in the NiO lattice [23]. This result is similar to the previous literature reported by Abelló et al. [26]. They reported that $Ni^{2+}$ ions occupy octahedral sites in the $Ni(Al)O_x$ phase when the sample was calcined at 500 °C, and occupy tetrahedral sites in the normal spinel $NiAl_2O_4$ when the sample was calcined at 900 °C.

The acidity of the catalysts is characterized by $NH_3$-TPD and the results are shown in Fig. 6. The desorption peaks of $NH_3$ for all catalysts appear in a very wide temperature range (90–430 °C), implying the presence of relatively weak acidic centers with broad distribution of acid strength. According to related literatures, it is known that a majority of Lewis acid sites originate from the $Al_2O_3$ support, while the incorporation of Ni into the $\gamma$-$Al_2O_3$ lattice or the formation of spinel $NiAl_2O_4$ could create some weak Lewis acidic sites on the Ni–Al catalysts [30–32].

### 3.2. Catalytic performance

The catalytic properties of various Ni–Al mixed oxides for the hydrodealkylation of 1,2,4-TMB are listed in Table 2. It is found that the catalytic activities of these catalysts are strongly influenced by changing the Ni/Al ratios and the calcination temperatures. Samples with higher Ni/Al ratios ($\geq$1/8) exhibit relatively high catalytic activity (above 52% conversion of 1,2,4-TMB), and the sample with a lower Ni/Al ratio (1/16) just gives a 28.5% conversion. Moreover, the two samples of $NiAl_8$-500 and $NiAl_{16}$-500 give much higher selectivity to xylene (or to BTX) than $NiAl_2$-500 and $NiAl_4$-500. Among them, $NiAl_8$-500 shows the highest conversion (62.3%) of 1,2,4-TMB and the highest selectivity to xylene (60.2%). The activity change with the time on stream over $NiAl_8$-500 (see Fig. 7a and Fig. 8a) shows that this catalyst possesses relatively high stability, and no obvious deactivation could be observed within 8 h reaction. Notably, both the TMB conversion and BTX yield even show a slight increase with extending reaction time. This result may suggest that the coordination environment or the state of active Ni species changes under the reaction atmosphere.

For the samples with the Ni/Al ratio of 1/8, increasing the calcination temperature from 500 °C to 700 °C or 900 °C could considerably decrease the activity of the catalysts (from 62.3% to 26.3% or 17.1%, see Table 3). The selectivity to BTX (or to xylene) decreases significantly with the increase in calcination temperatures, while 1,2,3-TMB and 1,3,5-TMB turn to the main products over the catalysts of $NiAl_8$-700 and $NiAl_8$-900. These results suggested that the

**Table 2**
Product distribution (wt%) of 1,2,4-TMB hydrodealkylation over the different Ni/Al ratio catalysts calcined at the temperature of 500 °C.

| Catalysts | Conv. (%) of 1,2,4-TMB | Sel. (%) to | | | Yield (%) | | | | | | |
|---|---|---|---|---|---|---|---|---|---|---|---|
| | | Ben | Tol | Xyl | Me | Ben | Tol | Xyl | 1,2,3-TMB | 1,3,5-TMB | TeMB |
| $NiAl_2$-500 | 52.0 | 1.33 | 3.25 | 21.7 | 35.8 | 0.69 | 1.69 | 11.3 | 1.04 | 0.80 | 0.72 |
| $NiAl_4$-500 | 53.8 | 5.26 | 10.1 | 39.0 | 20.1 | 2.83 | 5.44 | 21.0 | 1.79 | 1.52 | 0.98 |
| $NiAl_8$-500 | 62.3 | 0.58 | 7.93 | 60.2 | 8.19 | 0.36 | 4.94 | 37.5 | 4.29 | 5.27 | 1.65 |
| $NiAl_{16}$-500 | 28.5 | 0.32 | 5.30 | 55.4 | 2.22 | 0.09 | 1.51 | 15.8 | 4.17 | 3.36 | 1.16 |

Reaction conditions: total pressure 3.0 MPa, temperature 450 °C, LHSV = 1.1 $h^{-1}$, 1,2,4-TMP/$H_2$ = 1.9, T–O–S: 7 h.

**Table 3**
Product distribution (wt%) of 1,2,4-TMB hydrodealkylation over the catalysts (Ni/Al = 8) calcined at the different temperature.

| Catalysts | Conv. (%) of 1,2,4-TMB | Sel. (%) to | | | Yield (%) | | | | | | |
|---|---|---|---|---|---|---|---|---|---|---|---|
| | | Ben | Tol | Xyl | Me | Ben | Tol | Xyl | 1,2,3-TMB | 1,3,5-TMB | TeMB |
| $NiAl_8$-500 | 62.3 | 0.58 | 7.93 | 60.2 | 8.19 | 0.36 | 4.94 | 37.5 | 4.29 | 5.27 | 1.65 |
| $NiAl_8$-700 | 26.3 | 0.42 | 0.72 | 19.4 | 0.85 | 0.11 | 0.19 | 5.10 | 6.29 | 9.73 | 3.04 |
| $NiAl_8$-900 | 17.1 | 0.64 | 0.59 | 15.9 | 0.50 | 0.11 | 0.10 | 2.72 | 4.68 | 5.70 | 2.63 |

Reaction conditions: total pressure 3.0 MPa, temperature 450 °C, LHSV = 1.1 $h^{-1}$, 1,2,4-TMP/$H_2$ = 1.9, T–O–S: 7 h.

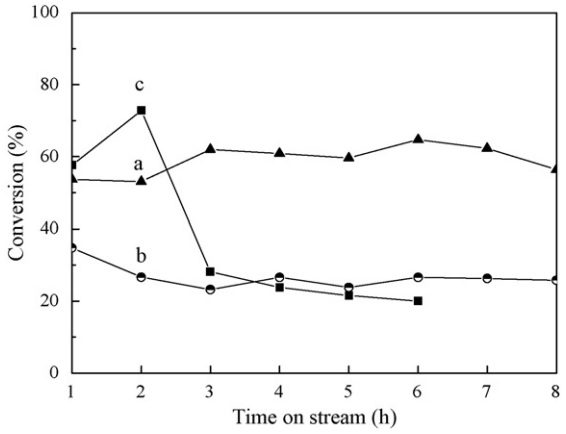


**Fig. 7.** 1,2,4-TMB conversion vs time on the $NiAl_8$-500 (a), $NiAl_8$-700 (b) and $NiAl_8$-700IMP (c).

isomerization of 1,2,4-TMB becomes the main reaction on the Ni–Al oxide catalysts calcined at higher temperatures.

The hydrodealkylation process of aromatic compounds includes two major reactions, hydrogenolysis and cracking reactions. Hence, one can envisage that two types of active sites should be required in order to achieve this catalytic transformation. By the study of kinetics and mechanisms of n-propylbenzene hydrodealkylation on silica-supported platinum catalysts and alumina materials,

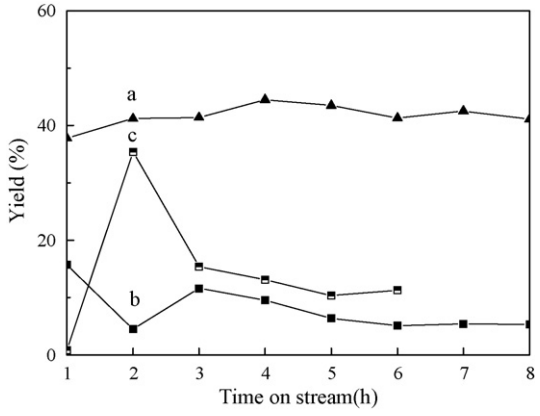


**Fig. 8.** BTX yield vs time on the $NiAl_8$-500 (a), $NiAl_8$-700 (b) and $NiAl_8$-700IMP (c).

Toppi et al. [33] proposed that these reactions occurs to a significant extent over both functions (active sites), metallic and acidic functions. For the model compound of 1,2,4-TMB, it was well known that different catalytic reactions including dealkylation, disproportionation and isomerization reaction may occur, which depends strongly on various parameters, such as the acidic properties of the catalysts and the operation conditions.

In this work, $H_2$-TPR characterization has confirmed that the reducibility of Ni–Al mixed oxides are varied with the change of Ni/Al ratios and the calcination temperatures. Samples calcined at lower temperatures (i.e., 500 °C) are easier to reduce compared to the samples calcined at higher temperatures. It should be pointed out here that all the Ni–Al mixed oxide catalysts have been pretreated in a reduced atmosphere ($H_2$) at 550 °C before the catalytic test. In this case, some reduced Ni species (e.g., Ni(0)) on the sample of $NiAl_8$-500 should appear, which originate from the reduction of a trace amount of NiO (nanoparticles), as well as the partial reduction of pseudo-spinel $NiAl_2O_4$. It was proposed previously that the reduction of surface nickel aluminate species would give rise to monodispersed nickel atoms, and the resultant Ni(0) atoms would remain closely associated with the alumina structure, thus may comprise a neighboring active sites (metallic Ni and Lewis acid site) [34].

As for the samples calcined at higher temperatures (i.e., $NiAl_8$-900), the formation of metallic Ni species (nickel nanoparticles or monodispersed nickel atoms) could be nearly neglected because these samples are more difficult to reduce under the pretreated conditions (i.e., $H_2$, 550 °C). Therefore, the excellent catalytic performance of $NiAl_8$-500 might be mainly assigned to the presence of both metallic Ni species and Lewis acid centers. We suppose that the formation of such neighboring active sites on the Ni–Al mixed oxide catalysts should play a synergic interaction in improving the catalytic activity and selectivity (to xylene).

In order to further understand the nature of the active sites on the reduced Ni–Al mixed oxide catalysts, the catalytic performance of the $NiAl_8$-700IMP, which is prepared by the impregnation method using $NiAl_8$-700 as support and nickel nitrate solution as nickel source, is also studied (Fig. 7). It can be seen that, the reduced $NiAl_8$-700IMP catalyst exhibits much higher activity than the sample of $NiAl_8$-700 during the initial 2 h, even higher than the sample of $NiAl_8$-500. However, with further prolonging the reaction time, the conversion of 1,2,4-TMB over $NiAl_8$-700IMP decreases rapidly from 72.8% (at 2 h) to 28.2% (at 3 h), which is very near to that of $NiAl_8$-700. Meanwhile, the yield of BTX on $NiAl_8$-700IMP is also quite similar to that on $NiAl_8$-700 after 3 h reaction (Fig. 8). The

XRD and $H_2$-TPR results (not shown here) suggest that a certain amount of metallic nickel particles could be formed on the surface of $NiAl_8$-700IMP after the reduction of NiO particles introduced by the impregnation method. Hence, the increase in the initial activity of the catalyst may suggest that the introduced metallic nickel particles are active for the hydrodealkylation. However, the fast deactivation of the $NiAl_8$-700IMP indicates that this kind of metallic nickel particles are unstable under the test reaction conditions. In fact, it is well known that NiO particles, which are weakly bound to support (e.g., $Al_2O_3$), are easy to reduce and sinter, thus resulting in the fast aggregation of nickel particles that promote carbon formation during the hydrogenation process [35]. On the other hand, it has been suggested that the highly dispersed nickel species (e.g., monodispersed nickel atoms originating from the reduction of surface nickel spinel phase) on the Ni–Al mixed oxides catalysts possess relatively high stability against sintering due to the relatively strong interaction between the nickel species and the supports ($Al_2O_3$ and/or $NiAl_2O_4$).

Moreover, it should be pointed out that some attention should be drawn on the formation of a side-product of methane. Some researchers have suggested that the presence of large amount of free nickel oxide over catalysts is not suitable for the hydrodealkylation reaction, and deep hydrogenation or cracking will easily occur to produce methane and other lower-carbon compounds [36]. Hence, it is very important to control the content of metallic Ni species as well as the intensity of the interaction between the metallic Ni species and the supports. Taking into account all the above, we may conclude here that the presence of a suitable amount of highly dispersed metallic Ni species and suitable Lewis acidic sites should be responsible for the unusual catalytic performance of $NiAl_8$-500 in the hydrodealkylation of 1,2,4-TMB.

## 4. Conclusion

The hydrodealkylation of 1,2,4-TMB has been investigated on partially reduced Ni–Al mixed oxide catalysts prepared by the co-precipitation method. The catalytic performance of these Ni–Al mixed oxides is considerably influenced by changing preparation parameters. The sample with a Ni/Al molar ratio of 1:8, which is calcined at 500 °C, shows the highest activity and selectivity to xylene. The relatively low calcination temperature is suitable for the formation of monodispersed metallic nickel species (Ni(0)), which originate from the partial reduction of surface pseudo-spinel $NiAl_2O_4$ phase. The excellent hydrodealkylation properties of this catalyst may be mainly assigned to the presence of a number of neighboring metallic Ni(0) atoms and Lewis acidic sites, which could simultaneously catalyze the hydrogenation and dealkylation processes of 1,2,4-TMB.

## Acknowledgements

This work is supported by Program for New Century Excellent Talents in University, and National Natural Science Foundation of China (20773050).

## References

[1] T.C. Tsai, S.B. Liu, I. Wang, Appl. Catal. A 181 (1999) 355–398.
[2] J.M. Serra, E. Guillon, A. Corma, J. Catal. 232 (2005) 342–354.
[3] Y.K. Lee, S.H. Park, H.K. Rhee, Catal. Today 44 (1998) 223–233.
[4] S.H. Park, H.K. Rhee, Catal. Today 63 (2000) 267–273.
[5] D. Shi, Z. Zhao, C. Xu, A. Duan, J. Liu, T. Dou, J. Mol. Catal. A 245 (2006) 106–113.
[6] A.G. Bhavani, D. Karthekayen, A.S. Rao, N. Lingappan, Catal. Lett. 103 (2005) 89–100.
[7] H.P. Roger, K.P. Moller, C.T. O'Connor, J. Catal. 176 (1998) 68–75.
[8] V.L. Barrio, P.L. Arias, J.F. Cambra, M.B. Güemez, B. Pawelec, J.L.G. Fierro, Appl. Catal. A 242 (2003) 17–30.
[9] B. Pawelec, P. Castan, J.M. Arandes, J. Bilbao, S. Thomas, M.A. Pen, J.L.G. Fierro, Appl. Catal. A 317 (2007) 20–33.
[10] C. Guimon, A. Auroux, E. Romero, A. Monzon, Appl. Catal. A 251 (2003) 199–214.
[11] P. Castan, B. Pawelec, J.L.G. Fierro, J.M. Arandes, J. Bilbao, Fuel 86 (2007) 2262–2274.
[12] K.V.R. Chary, P.V.R. Rao, V.V. Rao, Catal. Commun. 9 (2008) 886–893.
[13] H. Lu, H. Yin, Y. Liu, T. Jiang, L. Yu, Catal. Commun. 10 (2008) 313–316.
[14] P. Gayán, C. Dueso, A. Abad, J. Adanez, L.F. Diego, F.G. Labiano, Fuel 88 (2009) 1016–1023.
[15] S.R. Kirumakki, B.G. Shpeizer, G.V. Sagar, K.V.R. Chary, A. Clearfield, J. Catal. 242 (2006) 319–331.
[16] A. Al-Ubaid, E.E. Wolf, Appl. Catal. A 40 (1988) 73–85.
[17] J.C. Roddguez, E. Romeo, J.L.G. Fierro, J. Santamarfa, A. Monz, Catal. Today 37 (1997) 255–265.
[18] C. Resini, M.C.H. Delgado, L. Arrighi, L.J. Alemany, R. Marazza, G. Busca, Catal. Commun. 6 (2005) 441–445.
[19] N. Sahli, C. Petit, A.C. Roger, A. Kiennemann, S. Libs, M.M. Bettahar, Catal. Today 113 (2006) 187–193.
[20] Y. Cesteros, P. Salagre, F. Medina, J.E. Sueiras, Appl. Catal. B 25 (2000) 213–227.
[21] P.G. Savva, K. Goundani, J. Vakros, K. Bourikas, C. Fountzoula, D. Vattis, A. Lycourghiotis, Ch. Kordulis, Appl. Catal. B 79 (2008) 199–207.
[22] Y. Cesteros, P. Salagre, F. Medina, J.E. Sueiras, Chem. Mater. 12 (2000) 331–335.
[23] P. Kim, Y. Kim, H. Kim, I.K. Song, J. Yi, Appl. Catal. A 272 (2004) 157–166.
[24] H. Cui, M. Zayat, D. Levy, J. Non-Cryst. Solids 351 (2005) 2102–2106.
[25] D.C. Puxley, I.J. Kitchener, C. Komodromos, N.D. Parkyns, Stud. Surf. Sci. Catal. 16 (1983) 237–271.
[26] S. Abelló, D. Verboekend, B. Bridier, J. Pérez-Ramírez, J. Catal. 259 (2008) 85–95.
[27] P. Jeevanandam, Y. Koltypin, A. Gedanken, Mater. Sci. Eng. B 90 (2002) 125–132.
[28] S. Velu, V. Ramkumar, A. Narayanan, C.S. Swamy, J. Mater. Sci. 32 (1997) 957–964.
[29] A. Walsh, Y. Yan, M.M. Al-Jassim, S.-H. Wei, J. Phys. Chem. C 112 (2008) 12044–12050.
[30] F. Cavani, F. Trfiro, A. Vaccari, Catal. Today 11 (1991) 173–301.
[31] C.O. Arean, M.P. Mentruit, A.J.L. Lopez, J.B. Parra, Colloids Surf. A 180 (2001) 253–258.
[32] N. Wongwaranon, O. Mekasuwandumrong, P. Praserthdama, J. Panpranot, Catal. Today 131 (2008) 553–558.
[33] S. Toppi, C. Thomas, C. Sayag, D. Brodzki, F.L. Peltier, C. Travers, G. Djega-Mariadassou, J. Catal. 210 (2002) 431–444.
[34] D.C. Grenoble, J. Catal. 56 (1979) 32–39.
[35] G. Li, L. Hu, J.M. Hill, Appl. Catal. A 301 (2006) 16–24.
[36] V.M. Akhmedova, S.H. Al-Khowaiter, E. Akhmedov, A. Sadikhov, Appl. Catal. A 181 (1999) 51–61.